

OPEN ACCESS

EDITED BY
Janet Kubler,
California State University, Northridge,
United States

REVIEWED BY
Zhiguang Xu,
Ludong University, China
Pengbing Pei,
Shantou University, China

*CORRESPONDENCE
Xue Sun

Sunxue@nbu.edu.cn

[†]These authors contributed equally to this work and share first authorship

RECEIVED 26 May 2025 ACCEPTED 03 October 2025 PUBLISHED 21 October 2025

CITATION

Chu L, Ying X, Li M, Liu S, Xu N and Sun X (2025) Nitric oxide combined with abscisic acid contributes to high-temperature tolerance in macroalga *Gracilariopsis lemaneiformis. Front. Mar. Sci.* 12:1635506. doi: 10.3389/fmars.2025.1635506

COPYRIGHT

© 2025 Chu, Ying, Li, Liu, Xu and Sun. This is an open-access article distributed under the terms of the Creative Commons Attribution License (CC BY). The use, distribution or reproduction in other forums is permitted, provided the original author(s) and the copyright owner(s) are credited and that the original publication in this journal is cited, in accordance with accepted academic practice. No use, distribution or reproduction is permitted which does not comply with these terms.

Nitric oxide combined with abscisic acid contributes to high-temperature tolerance in macroalga *Gracilariopsis lemaneiformis*

Luke Chu[†], Xiao Ying[†], Mingyue Li, Shixia Liu, Nianjun Xu and Xue Sun^{*}

Key Laboratory of Aquacultural Biotechnology of Ministry of Education, School of Marine Sciences, Ningbo University, Ningbo, China

Introduction: The economic macroalga *Gracilariopsis lemaneiformis* is widely cultivated in China, yet high temperatures in the summertime constrain its cultivation period on China's southern coasts. Thus, it is of great significance to improve its heat tolerance. Nitric oxide (NO), a small signaling molecule, plays a vital role in resistance to abiotic stresses such as drought, salinity, and low/high temperature in higher plants. However, the role and underlying mechanism of NO in algae are still unclear.

Methods: Here, physiological assay and tandem mass tag (TMT)-labeled quantitative proteomics technique were used to elucidate the role of NO in resisting high-temperature-stressed *G. lemaneiformis*. And NO donor sodium nitroprusside (SNP), abscisic acid (ABA), NO scavenger, and ABA inhibitor were applied to explore the crosstalk of NO and phytohormone ABA.

Results: Physiological data showed that SNP promoted the algal growth (1.23-fold) and actual photosynthetic efficiency, yet reduced heat dissipation in *G. lemaneiformis* at 30°C. Proteomics results revealed that several KEGG pathways, including nitrogen metabolism, vitamin B6 metabolism, and glutathione metabolism, were significantly enriched after SNP treatment; meanwhile, a batch of differentially expressed proteins involved in carbohydrate metabolism and photosynthesis were also screened. In addition, SNP and/or ABA reduced malondialdehyde levels and promoted proline accumulation. Combined with the changes of endogenous NO and ABA levels, as well as their metabolic enzyme activities, it could be inferred that NO might act downstream of ABA.

Discussion/Conclusion: These findings demonstrate that NO and ABA can synergistically act against high-temperature stress in *G. lemaneiformis*. The present study will provide a valuable insight into understanding the mechanism of NO regulating high-temperature tolerance in macroalgae.

KEYWORDS

Gracilariopsis lemaneiformis, nitric oxide, high temperature, abscisic acid, proteomics

1 Introduction

The economic macroalga Gracilariopsis lemaneiformis (Rhodophyta, Gracilariales) is mainly used as raw materials for agar production and baits for abalone. In addition, G. lemaneiformis can effectively remove nitrogen and phosphorus from the environment, displaying a strong ability to reduce seawater eutrophication (Yu and Yang, 2008). Wild G. lemaneiformis is a temperate seaweed that naturally inhabits the intertidal zone of northern China, with a suitable growth temperature from 10°C to 23°C. Currently, the bred G. lemaneiformis species 981 and Lulong No. 1 with the characteristics of fast-growing and high-temperature resistance (26°C or 27°C) are widely cultivated in the southern and northern coasts of China. In general, cultivation of G. lemaneiformis is adopted in an inter-regional mode, that is, the northern seaweeds need to be transported to the south for winter, and the southern seaweeds are shipped to the north for the summer. High temperatures in the summertime are an important factor limiting the growth period of G. lemaneiformis in southern China. Excessive temperature can easily cause algal damage or even decay, so there is an urgent need for research on the protection of algae under high temperature and breeding species that can resist heat stress.

Nitric oxide (NO), as a ubiquitous gaseous signaling molecule, executes its multifunction in the whole life process of plants, including seed germination, root morphogenesis, and programmed cell death (Kopyra and Gwózdz, 2004). Under abiotic stress such as heat and drought, the accumulation of NO is a universal phenomenon in plants, which results in the improvement of stress resistance (Bouchard and Yamasaki, 2008; Xiong et al., 2012). Similarly, the application of NO donors has confirmed the high-temperature resistance of NO-for example, exogenous sodium nitroprusside (SNP, a NO donor) can reduce the oxidative stress in wheat by stimulating photosynthesis and increasing osmolyte accumulation under heat conditions (Sehar et al., 2023). On the contrary, the application of NO scavenger 2-(4carboxyphenyl)-4,4,5,5-tetramethylimidazoline-1-oxyl-3-oxide (cPTIO) has weakened the protective effect of NO against heat stress in tomato seedlings (Siddiqui et al., 2017).

NO plays a pivotal role throughout the entire life process of organisms; thereby, its source has attracted much attention. A high NO level mediated by exogenous NO is predominantly maintained through increasing NR rather than NOS-like activity in cold-stored peach (Tian et al., 2020). Nonetheless, exogenous NO significantly promoted the endogenous NO synthesis by activating NOS activity in cold-stored *Abelmoschus esculentus* (Sun et al., 2021). Furthermore, NO interacts with phytohormones such as abscisic acid (ABA) and gibberellic acid, collectively regulating the entire life processes of plants (Song et al., 2008; Zhang et al., 2023b). Among the numerous phytohormones, the relationship between NO and ABA is one of the most extensively studied (Wang et al., 2020; García-Mata and Lamattina, 2001).

In algae, NO also plays an essential role in stress response, such as stimulation of growth under various stresses, photo-protection or acclimation under high light stress, and action as signaling molecules in copper stress (Kumar et al., 2015). However, the role

and underlying mechanism of NO against high-temperature stress of *G. lemaneiformis* is unclear. Hence, this study first investigated the effects of exogenous NO at the physicochemical and protein profiling levels in high-temperature-stressed *G. lemaneiformis* and then explored the interaction between NO and ABA. These results elucidated the potential mechanisms by which NO exerts its effects on heat stress, thereby contributing to the theoretical understanding of NO's role in macroalgae, aiming to serve as a reference for the development of thermotolerant *G. lemaneiformis* strains.

2 Materials and methods

2.1 Materials and culture conditions

The seaweed *G. lemaneiformis* 981 was collected from the aquaculture base of Xiapu (26°65′ N, 119°66′ E), Fujian Province. In the laboratory, the sediment and attachments on the algal surface were washed off, and then healthy thalli (approximately 7–10 cm) were cultured for adaptation in a salinity of 25 psu artificial seawater enriched with Provasoli medium (Provasoli, 1968). The preculture was carried out at 23°C with a photoperiod of 12-h light and 12-h dark and light intensity of 45 μ mol photons/(m²-s).

2.2 Experimental design

All of the experiments were conducted at 30°C after 3 days of preculture, and the rest of the culture conditions were the same as the aforementioned adaptive cultivations except for temperature. In the NO supplementation experiments, healthy thalli were cultivated at 30°C without SNP addition as the control group (CK group), and exogenous 400 μ mol/L SNP was applied in the SNP group. To explore the crosstalk of NO and ABA, the other four groups were designed, including 50 μ mol/L ABA (ABA group), 400 μ mol/L SNP + 50 μ mol/L ABA (SNP + ABA group), 50 μ mol/L ABA + 10 μ mol/L cPTIO (NO scavenger) (ABA + cPTIO group), and 400 μ mol/L SNP + 20 μ mol/L fluridone (Flu, ABA inhibitor) (SNP + Flu group). The quantitative proteomics and the most physicochemical indicators such as malondialdehyde (MDA) content and 9-cisepoxycarotenoid dioxygenase (NCED) activity were analyzed at 48 h. Each treatment was performed in triplicate.

2.3 Determination of growth and chlorophyll fluorescence parameters

Fresh weight (FW) was accurately measured to calculate the relative growth rate (RGR) of *G. lemaneiformis* according to Ji et al. (2019). The calculation formula is as follows: RGR (%/day) = ($\ln W_t$ - $\ln W_0$)/ $t \times 100$ %, where W_t and W_0 refer to the weight on t and t0 days, respectively; t represents the time (day).

The chlorophyll fluorescence parameters, including the actual photochemical efficiency of PSII [Y(II)] and non-photochemical quenching (NPQ), were measured at 0, 24, 48, and 72 h after

treatment using a portable modulated pulse fluorescence analyzer (AquaPen-PAP-P100, FESTO, Czech).

2.4 TMT-labeled quantitative proteomics analysis

After treatment for 48 h, samples of the CK and SNP groups were collected and analyzed with a TMT stable isotope labeling technique combined with liquid chromatography (Ultimate 3000 RSLCnano, Thermo, USA) and mass spectrometry (Exploris 480, Thermo, USA) in Micrometer Biotech (Hangzhou, Zhejiang, China). The whole experimental process was according to Lin et al. (2022) with minor modifications. Approximately 0.1 g of the samples was ground into powder and mixed in protein lysis buffer to extract the total proteins. Subsequently, the extracted proteins were digested into peptides and were desalted on a C18 SPE column (Phenomenex, USA). After being labeled with a TMT kit (Thermo Fisher Scientific, Waltham, MA, USA), the vacuumdried aliquots (approximately 100 µg) of peptides were mixed and fractionated on a C18 column. Finally, the peptides were drained with a vacuum concentrator (SPD111V-230, Thermo, USA) and grouped into six fractions for the proteomics assay.

2.5 Protein annotation and enrichment analysis

The MS raw data were analyzed using Maxquant software (v.1.5.2.8). Trypsin/P was specified as a cleavage enzyme, allowing up to two missing cleavages. The mass tolerance for precursor ions was set as 10 ppm in the first search, and the mass tolerance for fragment ions was set as 0.02 Da. The cutoff of the global false discovery rate (FDR) for peptide and protein identification was set to \leq 0.01. The differentially expressed proteins (DEPs) were considered when the fold changes were \geq 1.2 (SNP/CK \geq 1.2) or \leq 0.83 (SNP/CK \leq 0.83), with *P*-value <0.05.

To classify the DEPs' function, Gene Ontology (GO) and Kyoto Encyclopedia of Genes and Genomes (KEGG) enrichment analyses were performed. All DEPs were subjected to GO and KEGG databases, and Fisher's exact test was used for statistical analysis. The GO terms and KEGG pathways with P-value <0.05 were considered significantly enriched.

2.6 Western blot validation

To verify the proteomics results, two DEPs of NR and phosphoglucose mutase 3 (PGM3) were selected for western blot analysis. At 12, 24, 48, and 72 h, the total proteins were extracted by using RIPA lysis buffer and quantified by using the Enhanced Bicinchoninic Acid (BCA) Protein Assay Kit (Biyuntian, Shanghai). After that, the proteins were separated by 12.5% SDS-PAGE, and immunoblotting analysis was carried out. Among these, NR rabbit polyclonal antibodies were purchased from Agrisera

(Sweden), and PGM3 rabbit polyclonal antibodies were prepared in the previous study (Chen et al., 2022). The mouse anti-beta-actin antibody (Boosen, Beijing) was used as an internal reference.

2.7 Determination of MDA and proline contents

To determine the MDA and proline contents, approximately 0.1 g thalli was powdered in liquid nitrogen and dissolved in MDA and proline extracting solutions, respectively. After vortexing and centrifugation, the supernatants were used for testing the content following the instructions of the MDA assay kit (Jiancheng, Nanjing) and proline assay kit (Soleibao, Beijing).

2.8 Measurement of NO content and NR and NOS activities

For NO content determination, approximately 0.1 g algal powder was extracted in 1 mL NO extracting solution and mixed thoroughly. After centrifugation at $8,000 \times g$ for 10 min at 4°C, the supernatants were soaked in boiling water for 5 min. Then, they were centrifuged again, and the supernatants were used to detect the NO content. The NO content was measured using the nitric oxide (NO) content determination kit (Greasy, Suzhou).

In NR activity analysis, the samples (0.1 g) were treated with induction of NR enzyme activity before grinding; then, the samples were dissolved in 1 mL NR extracting solution. In NOS-like activity assay, the PBS (pH 7.2) extraction solution was adopted. After thorough shaking and mixing, the mixtures were centrifuged at $8,000 \times g$ for 10 min at 4°C, and the supernatants were collected for NR and NOS activity measurement, respectively. Both NR and NOS activities were performed using the corresponding assay kits (Jiancheng, Nanjing).

2.9 Determination of ABA content and NCED activity

The ABA content and NCED activity were determined using the corresponding ELISA detection kits (Sinovac, Shanghai). According to the instructions, linear regression curves of ABA content and NCED activity were fitted with the standard substance concentrations as the horizontal axis and corresponding OD values as the vertical axis, respectively. Afterward, the ABA content and the NCED activity were obtained according to the curve equations.

2.10 Data statistics and analysis

The data were processed by using Microsoft Office Excel 2019 and were expressed as mean \pm standard deviation (mean \pm SD). The statistical significance of the data was established using SPSS 20. One-way ANOVA and Duncan's test were used to analyze the

statistical significance of the data at a level of P <0.05. The software Origin 2021 was used for drawing.

3 Results

3.1 The effects of SNP on growth and chlorophyll fluorescence characteristics

The effects of SNP on the relative growth rate of *G. lemaneiformis* are shown in Figure 1A. On day 3, SNP promoted algal growth, and the RGR was increased to 1.23-fold relative to that of the CK group. Y (II) was likewise increased to 1.18- and 1.09-fold after SNP supply at 24 and 72 h compared to the CK group (Figure 1B). Differently from Y (II), NPQ was downregulated from 0.17- to 0.45-fold after SNP treatment during the 72-h time course (Figure 1C). The results indicated that SNP enhanced the photosynthetic efficiency and reduced the heat dissipation, resulting in the accelerated growth rate of *G. lemaneiformis* under high-temperature stress.

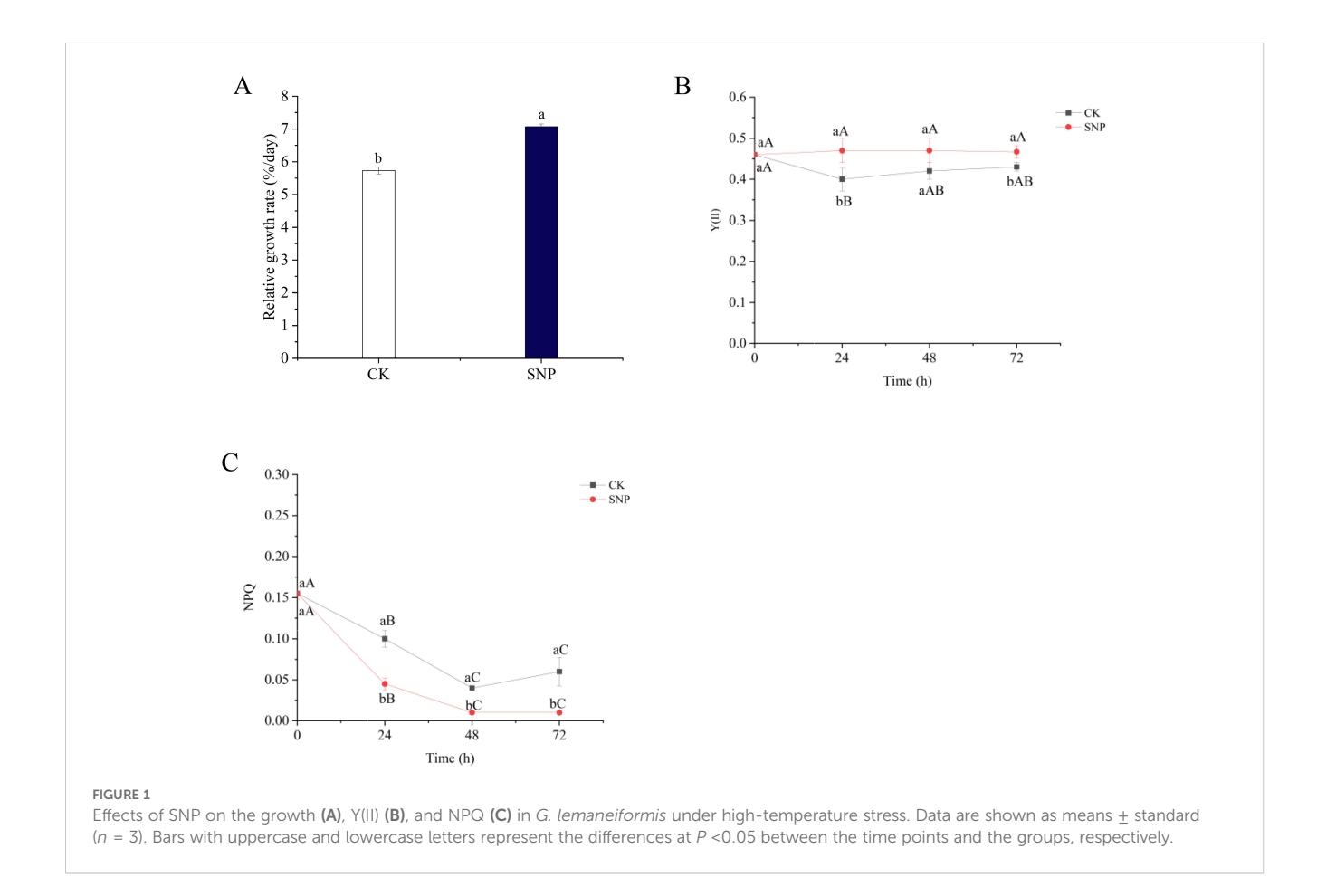
3.2 Proteomics results and validation

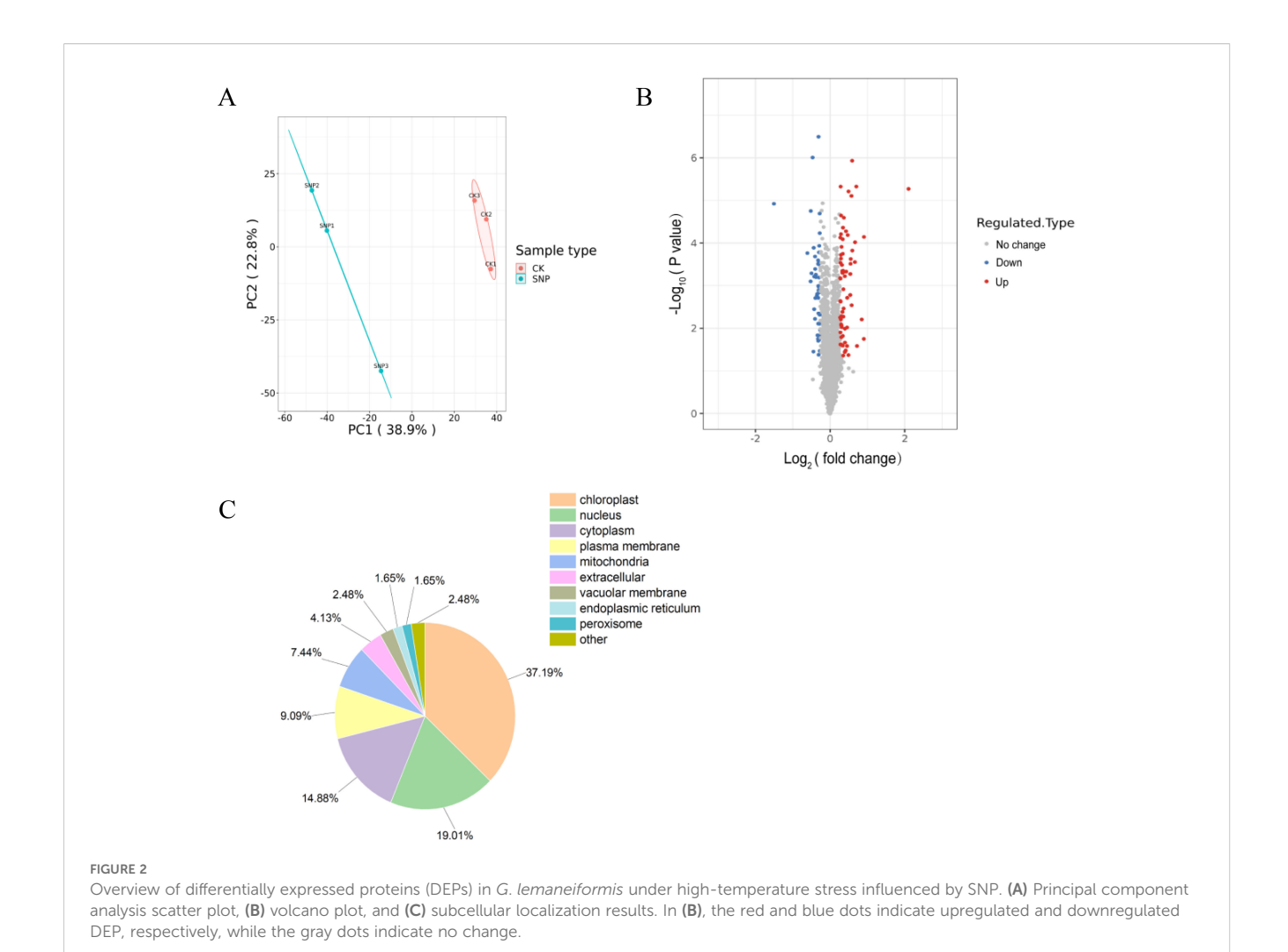
To explore the protein expression profiles of *G. lemaneiformis* influenced by SNP, a quantitative proteomics analysis was

performed. In this proteomics result, 303,986 secondary spectra were generated, and 40,882 spectra were matched after searching the protein database. By spectral analysis, 16,183 unique peptides and 3,524 proteins were identified, of which 3,156 proteins were quantified. Principal component analysis (PCA) was performed to describe the proteome differences between the SNP and CK groups. The principal components PC1 and PC2 of the total variance accounted for 38.90% and 22.80%, respectively, displaying a clear separation on the two-dimensional graph (Figure 2A). The clear separation results manifested that the protein expression levels were significantly altered after SNP treatment.

Among the quantified proteins, 71 upregulated and 50 downregulated DEPs were screened in the SNP group vs. the control group (Figure 2B). Out of the 121 DEPs, the majority were found in chloroplasts (37.19%), followed by nuclei (19.01%) and cytoplasm (14.88%), as revealed by subcellular structure prediction (Figure 2C). Additionally, a small proportion of DEPs was located in the endoplasmic reticulum (1.65%) and peroxisomes (1.65%).

To verify the TMT-based quantitative proteomics results, two DEPs of NR and PGM3 were selected for western blot analysis (Supplementary Figure S1). After SNP addition, the NR protein levels were increased to 1.60- and 1.45-fold compared to the CK group at 24 and 48 h, respectively. Similarly, the PGM3 protein levels were consistently higher than that in the CK group, with changes from 1.26- to 1.52-fold during the 72-h time course.





Moreover, the expression of the two proteins at 48 h was upregulated to 1.45- and 1.31-fold, respectively, which was basically consistent with the proteomics results (both 1.22-fold).

3.3 GO and KEGG enrichment analysis of the DEPs affected by SNP

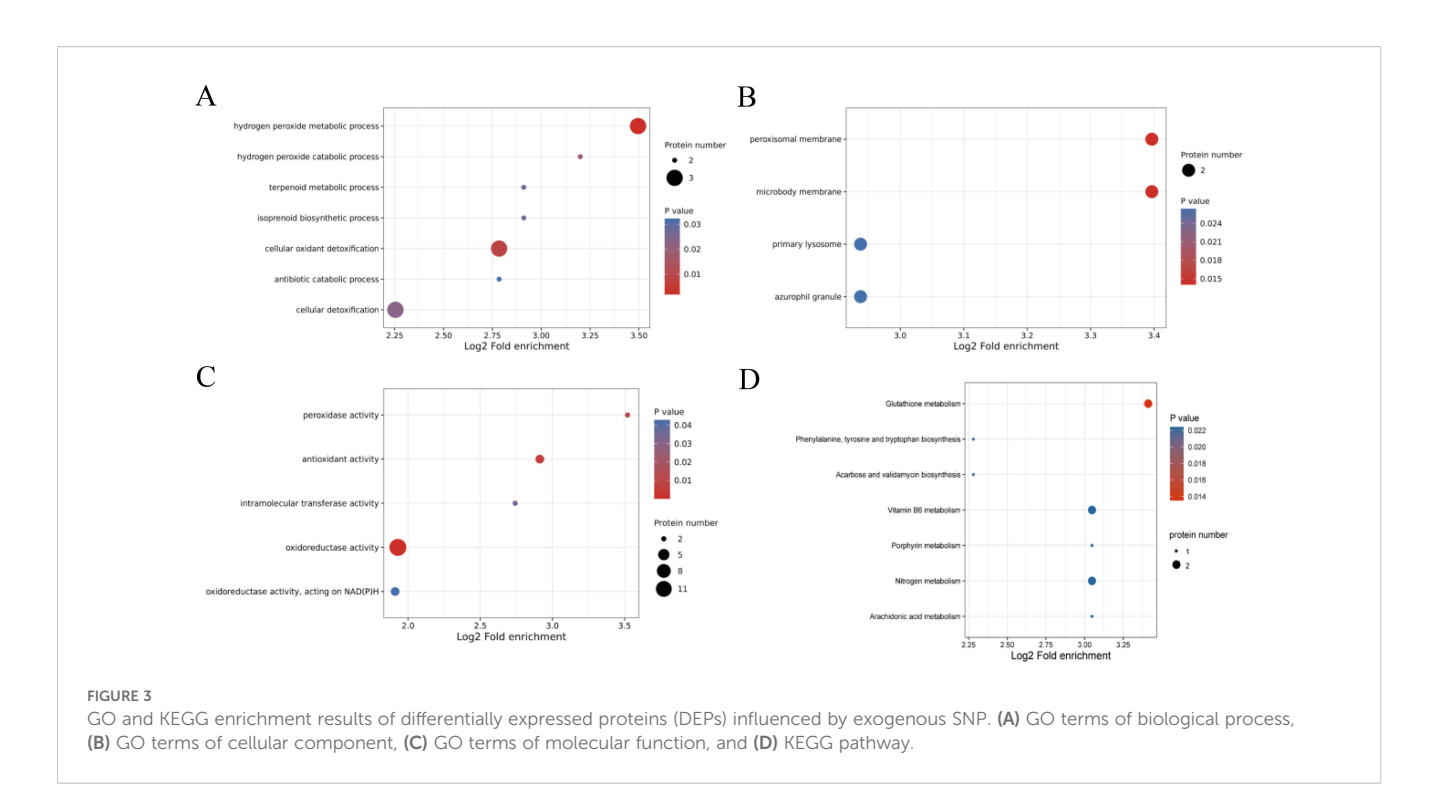
To analyze the functions of these DEPs, GO and KEGG enrichment analyses were conducted. In the three categories of GO database, six DEPs were enriched in biological processes (BP), being highly enriched in the hydrogen peroxide metabolic process, cellular oxidant detoxification, and cellular detoxification terms (Figure 3A); four DEPs were enriched in cellular components (CC), including peroxisomal membrane, microbody membrane, primary lysosome terms, and azurophil granule (Figure 3B); and 15 DEPs were observed in molecular functions (MF), among which 13 DEPs were significantly enriched in oxidoreductase activity terms (Figure 3C).

In the enriched KEGG analysis, the pathways of nitrogen metabolism (map00910) and vitamin B6 metabolism (map00750) were upregulated, while glutathione metabolism (map00480) was

downregulated (Figure 3D). In addition, DEPs were also significantly enriched in phenylalanine, tyrosine, and tryptophan biosynthesis (map00400), acarbose and validamycin biosynthesis (map00525), porphyrin metabolism (map00860), and arachidonic acid metabolism (map00590) pathway.

3.4 Enriched KEGG and other metabolism pathways regulated by SNP

Of the seven significantly enriched KEGG pathways, nitrogen metabolism, vitamin B6 metabolism, and glutathione metabolism were further analyzed. Nitrogen metabolism is the foundation of plant growth and development, and it also affects plant adaptability and tolerance to stress. In this study, SNP stimulated nitrogen metabolism under high-temperature conditions. Two key proteins including nitrate reductase (NR, EC:1.7.1.1 1.7.1.2 1.7.1.3, A0A2V3J6L8) and ferredoxin-nitrite reductase (NirA, EC:1.7.7.1, A0A2V3J4B2) were upregulated to 1.22- and 1.51-fold compared to the control group after SNP treatment, respectively. NR catalyzes nitrate to generate nitrite, while NirA is responsible for the conversion of nitrite to ammonia. Thus, it can be seen that



exogenous SNP improved the nitrogen metabolism at high temperatures (Figure 4A, Table 1).

Vitamin B6 exists widely in the forms of pyridoxine, pyridoxal, and pyridoxamine in plants and animals. In the pathway of vitamin B6 metabolism, the expression level of pyridoxal 5′-phosphate synthase (PPOX, EC:1.4.3.5, A0A2V3ICY3), responsible for the interconversion between pyridoxal and pyridoxine, was upregulated to 1.40-fold (Figure 4B, Table 1). Notably, phosphoserine transaminase (PSAT, EC:2.6.1.52, A0A2V3IMC5), involved in the transformation of O-phospho-4-hydroxy-L-threonine and 2-oxo-3-hydroxy-4-phosphobutanoate, was upregulated to 4.29-fold. In addition, PSAT was also related to the synthesis of serine.

Unlike the previous upregulated enrichment pathways, glutathione metabolism was downregulated. Two peroxiredoxin 6 (Prdx6) proteins (EC:1.11.1.7, A0A2V3IUC8 and A0A2V3ILF0) in the glutathione metabolism pathway were downregulated to 0.70-and 0.35-fold in the SNP group compared to the CK group (Table 1), though Prdx6 is involved in countering oxidative stress (Rahaman et al., 2024).

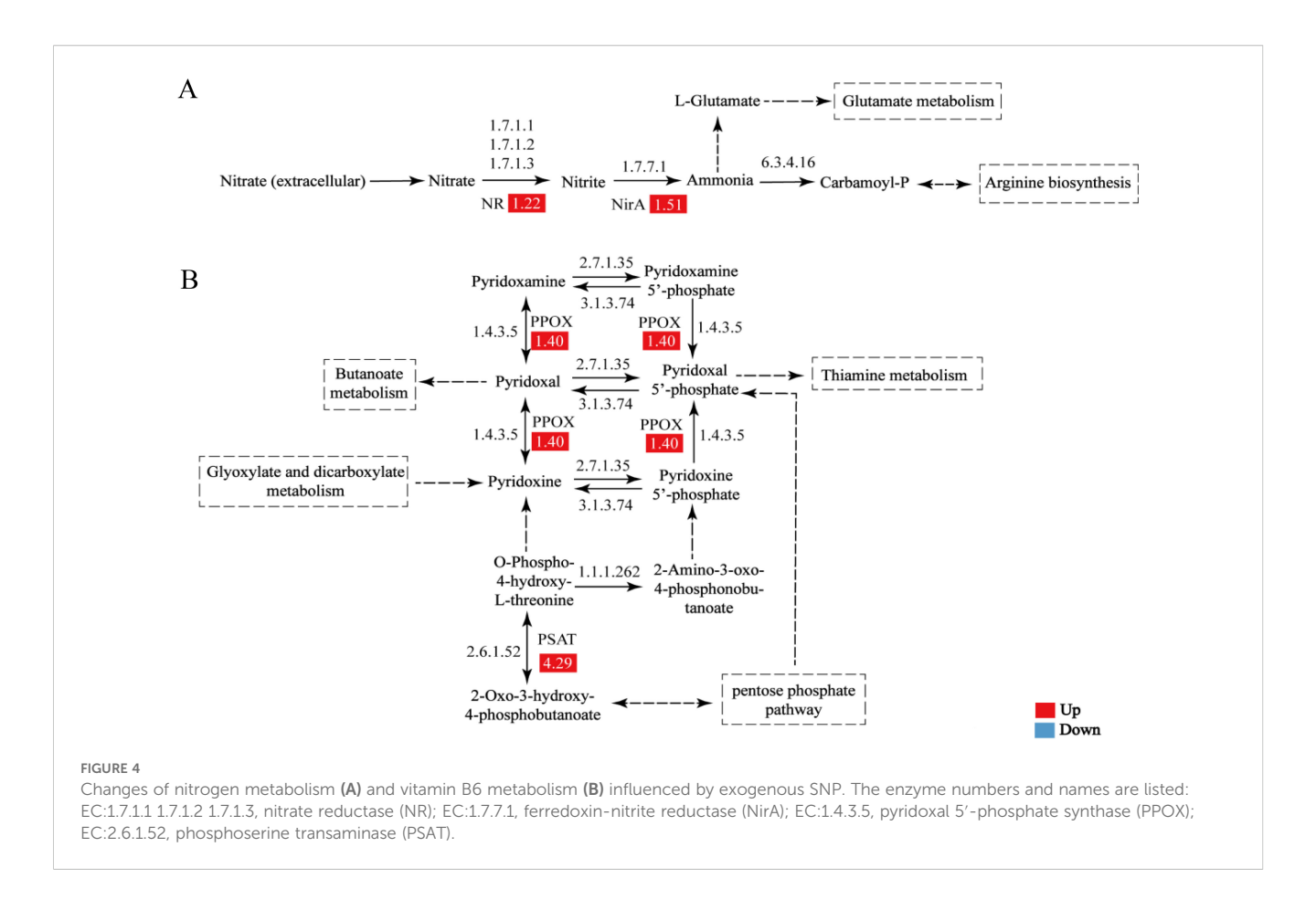
Except for those DEPs in the enrichment pathways, some DEPs in other metabolism pathways were also identified. Among photosynthesis-related proteins, five upregulated and two downregulated DEPs were observed. These proteins were mainly associated with phycobiliprotein, chloroplasts, photorespiration, and synthesis of photosynthetic pigments (Table 1), including phycoerythrobilin/ferredoxin oxidoreductase (PebB, A0A2V3IZJ2, 1.37-fold), fucoxanthin-chlorophyll a-c binding protein A (FCPA, A0A2V3IPQ1, 1.23-fold), geranylgeranyl pyrophosphate synthase (GGPPS, A0A2V3IFL6, 1.21-fold), phospho-2-dehydro-3-deoxyheptonate aldolase (A0A2V3ILE3, 1.21-fold), phosphoglycolate phosphatase 1B (PGLP, A0A2V3J238, 1.21-

fold), and geranylgeranyl diphosphate reductase (GGDR, A0A2V3J5V9, 0.77-fold).

Carbohydrate metabolism is an important basic metabolism in plants, providing the necessary carbon frame and energy. In our study, a total of seven DEPs were identified as involved in carbohydrate metabolism (Table 1). As part of pyruvate dehydrogenase complex, dihydrolipoyl dehydrogenase (DLD) protein was upregulated (A0A2V3IHR3, 1.35-fold), while the malic enzyme related to the Calvin cycle was slightly downregulated (A0A2V3J6D4, 0.81-fold). The rest were five proteins related to glucose metabolism (Table 1). Among them, three DEPs of mannosylglycerate synthase (MGS, A0A2V3IRZ7, 1.46-fold), phosphomannomutase/phosphoglucomutase (PMM/ PGM, A0A2V3IKF4, 1.22-fold), and fructose-1,6-bisphosphatase (FBP, A0A2V3IS48, 1.21-fold) were upregulated, while two DEPs of GDP-fucose transporter 1 (GFT1, A0A2V3IIV5, 0.83-fold) and alpha-glucosidase 2 (malZ2, A0A2V3IDQ1, 0.81-fold) were downregulated.

3.5 Effects of SNP and/or ABA on growth and MDA and proline contents

To investigate the interaction of SNP and ABA against high-temperature stress, the effects of SNP and/or ABA and their scavenger/inhibitor on growth were illustrated (Figure 5A). The RGR of G. lemaneiformis in SNP and SNP + ABA groups was increased to 1.21-and 1.18-fold at the 5th day compared to the control group, respectively. The effects of ABA on algal growth seemed to be limited (P > 0.05) at 30°C, whereas ABA showed a significant promoting effect in G. lemaneiformis at 33°C (Sun et al., 2022). The



combination of Flu with SNP decreased the algal RGR to 0.60-fold compared to SNP alone. Similarly, ABA co-application with NO scavenger also reduced the algal RGR to 0.84-fold relative to ABA alone. The above-mentioned results suggested that ABA was involved in the regulation of growth promotion mediated by NO, and a positive crosstalk between NO and ABA could be deduced from the results after the application of NO scavenger or ABA inhibitor.

Compared to the CK group, SNP, ABA, and SNP + ABA treatments all reduced the MDA contents to 0.87-, 0.89-, and 0.82-fold in *G. lemaneiformis*, respectively (Figure 5B). Notably, the combination of SNP and ABA demonstrated the most significant effect among the three treatments. Moreover, compared to ABA or SNP alone, the addition of cPTIO or Flu significantly increased the MDA contents to 1.22- and 1.23-fold, respectively. From these results, it can be seen that SNP and ABA had a synergistic effect on mitigating membrane lipid damage caused by high temperature in *G. lemaneiformis*, while the use of NO scavenger or ABA inhibitor counteracted the positive effects.

Contrary to the impacts of MDA, SNP and/or ABA elevated the proline levels (Figure 5C). Notably, the combination of SNP and ABA exhibited the most significant improvement on proline accumulation with 1.44-fold, while individual ABA was the least (1.13-fold). Furthermore, the proline contents in the ABA + cPTIO group were decreased to 0.86-fold relative to the ABA group, while no significant changes were detected between the SNP and SNP + Flu groups. Consequently, it can be inferred that ABA could synergistically act on the accumulation of proline with SNP, but

its inhibition did not significantly affect the positive effects of SNP, suggesting that ABA might function upstream of the NO signaling pathway.

3.6 Effects of SNP and/or ABA on internal NO and ABA synthesis

To explore the crosstalk mechanism between ABA and NO, the NO contents and its two metabolic enzyme activities were analyzed (Figures 6A-C). The NO contents and NR activities were all increased by SNP, ABA, and their combination, with the maximum of 1.18- and 1.94-fold relative to the CK group, respectively. Additionally, ABA showed maximum enhancement of the NR activity. On the other hand, the increased NO contents and NR activities by SNP were reduced after supply with Flu, while ABA and ABA + cPTIO had no significant effects on NO levels and NR activities. As for another NO synthesis enzyme of NOS, its activities showed no significant change among all of the groups. Thus, the promotion of NO accumulation in G. lemaneiformis might be NR dependent. These results indicated that ABA stimulated the accumulation of endogenous NO to a certain extent, and NO scavenger did not reduce the accumulation of NO induced by ABA (P > 0.05), yet ABA inhibitor slightly reduced the accumulation of NO promoted by SNP (P < 0.05).

To further examine the underlying mechanism between ABA and NO, the ABA content and its metabolic enzymes were also

TABLE 1 DEPs involved in the metabolisms affected by SNP.

Protein ID	Protein annotation	SNP/CK	<i>P</i> -value		
Significantly enriched KEC	GG pathways	'	·		
Nitrogen metabolism					
A0A2V3J6L8	Nitrate reductase (NR)	1.22	1.89E-04		
A0A2V3J4B2	Ferredoxin-nitrite reductase, chloroplast (NirA)	1.51	1.50E-04		
Vitamin B6 metabolism					
A0A2V3IMC5	Phosphoserine transaminase (PSAT)	4.29	5.36E-06		
A0A2V3ICY3	Pyridoxal 5'-phosphate synthase (PPOX)	1.40	4.26E-02		
Glutathione metabolism					
A0A2V3IUC8	Peroxiredoxin 6 (Prdx6)	0.70	1.77E-05		
A0A2V3ILF0	Peroxiredoxin 6 (Prdx6)	0.35	1.19E-05		
Phenylalanine, tyrosine, and tryptophan biosynthesis					
A0A2V3ILE3	Phospho-2-dehydro-3-deoxyheptonate aldolase (aroG)	1.21	6.63E-04		
Acarbose and validamycin bios	synthesis				
A0A2V3J638	2-epi-5-epi-valiolone synthase	0.79	1.46E-02		
Porphyrin metabolism					
A0A2V3IPS7	Putative threonine-phosphate decarboxylase (cobD)	1.22	2.36E-03		
Arachidonic acid metabolism	'	'			
A0A2V3IU57	Carbonyl reductase [NADPH] 2 (CBR2)	0.73	3.53E-02		
Other metabolism pathwa	ays				
Photosynthesis					
A0A2V3IZJ2	Phycoerythrobilin/ferredoxin oxidoreductase (PebB)	1.37	9.57E-03		
A0A2V3IPQ1	Fucoxanthin-chlorophyll a-c binding protein A, chloroplast (FCPA)	1.23	1.62E-02		
A0A2V3IFL6	Geranylgeranyl pyrophosphate synthase, chloroplast (GGPPS)	1.21	1.25E-02		
A0A2V3J238	Phosphoglycolate phosphatase 1B, chloroplastic (PGLP)	1.21	5.58E-03		
A0A2V3J5V9	Geranylgeranyl diphosphate reductase (GGDR)	0.77	5.53E-04		
Carbohydrate metaboli	sm				
A0A2V3IHR3	Dihydrolipoyl dehydrogenase (DLD)	1.35	4.69E-04		
A0A2V3J6D4	Malic enzyme	0.81	1.28E-03		
A0A2V3IRZ7	Mannosylglycerate synthase (MGS)	1.46	3.07E-04		
A0A2V3IKF4	Phosphomannomutase/phosphoglucomutase (PMM/PGM)	1.22	2.25E-05		
A0A2V3IS48	Fructose-1,6-bisphosphatase (FBP)	1.21	6.82E-04		
A0A2V3IIV5	GDP-fucose transporter 1 (GFT1)	0.83	3.40E-02		
A0A2V3IDQ1	Alpha-glucosidase 2 (malZ2)	0.81	3.15E-04		
Antioxidant system	Antioxidant system				
A0A2V3IG38	L-ascorbate peroxidase 5, peroxisomal (APX)	1.47	2.37E-04		
A0A2V3J221	Peroxisomal membrane protein 2 (PXMP2)	0.83	1.42E-03		
A0A2V3IF93	Thioredoxin (Trx)	0.80	2.54E-04		

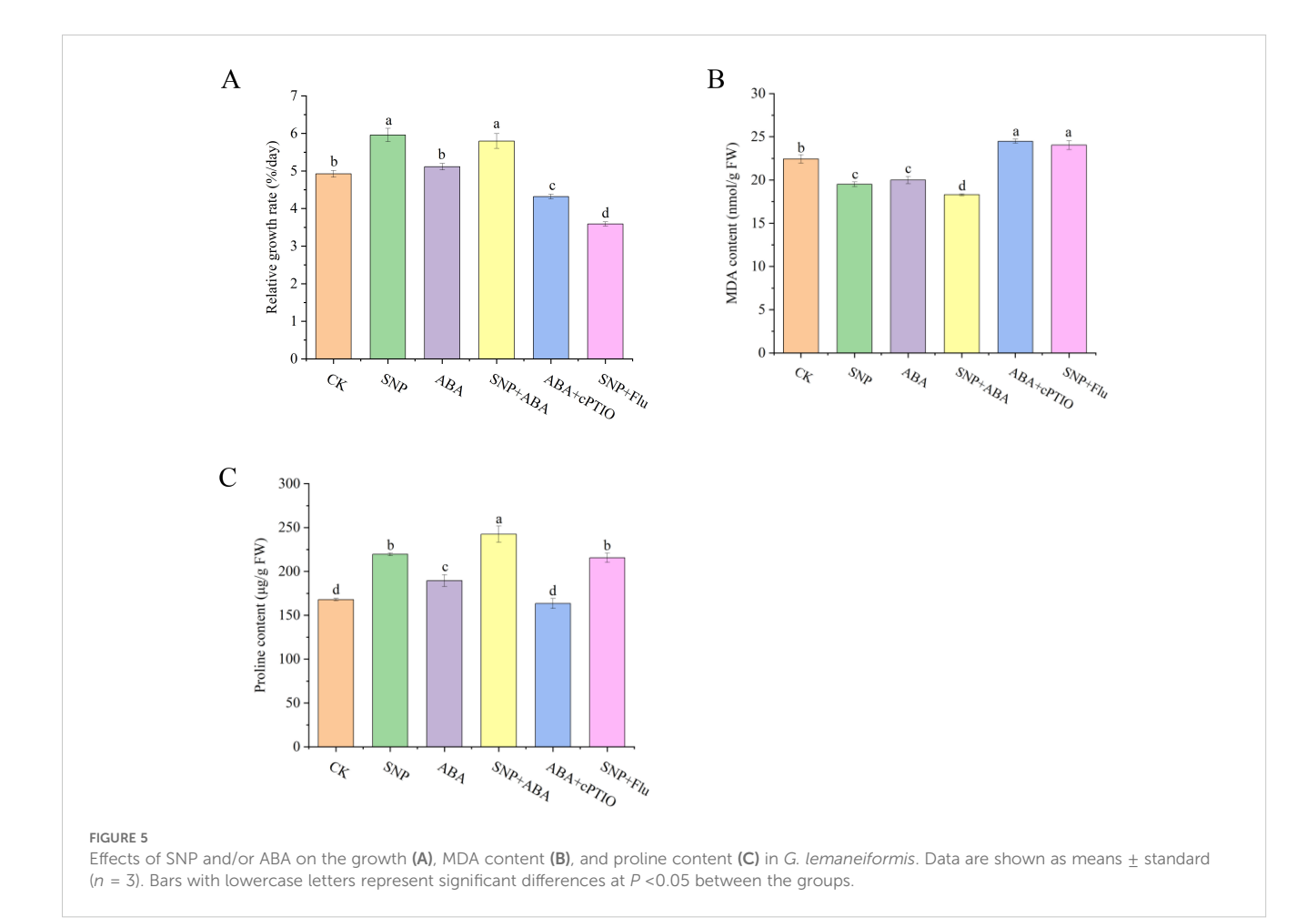
(Continued)

TABLE 1 Continued

Protein ID	Protein annotation	SNP/CK	P-value		
Ribosome biogenesis					
A0A2V3J354	30S ribosomal protein S21	1.32	2.16E-02		
A0A2V3J4A9	50S ribosomal protein L10	1.28	5.33E-03		
A0A2V3IU24	Ribosomal protein S6 kinase beta	1.23	2.41E-02		
A0A2V3IJV6	Ribosomal silencing factor RsfS	0.81	1.07E-03		
A0A2V3J5W9	Ribosome maturation factor RimP	0.78	1.72E-03		
ABA-related signaling pathway					
A0A2V3J3A0	Phosphatase 2C 35 (PP2C)	1.22	2.39E-02		

determined (Figures 6D, E). At the high temperature of 30°C, exogenous ABA enhanced the endogenous ABA levels (1.33-fold), while treatment with cPTIO decreased these levels, indicating that clearance of NO reduced the endogenous ABA contents. Beyond expectation, SNP and co-treatment with ABA or Flu did not demonstrate a significant difference at the ABA level (P > 0.05). Regarding the NCED enzyme, one ABA synthetase, SNP and ABA alone or in combination all contributed to stimulating its activity. More specifically, NCED activity exhibited the most substantial

increase in the ABA group (1.48-fold) and then followed by that in the SNP + ABA group (1.27-fold) and the SNP group (1.15-fold). The NCED activity was inhibited to 0.78-fold after addition of NO scavenger compared to ABA treatment alone. Similarly, the NCED activity was restrained in the SNP + Flu group (0.71-fold) compared to the SNP group. Combined with the changes of ABA content and NCED activity, it can be concluded that NO scavenger reduced the accumulation of endogenous ABA and its metabolic enzyme activity, indicating that NO might be involved in ABA metabolism.



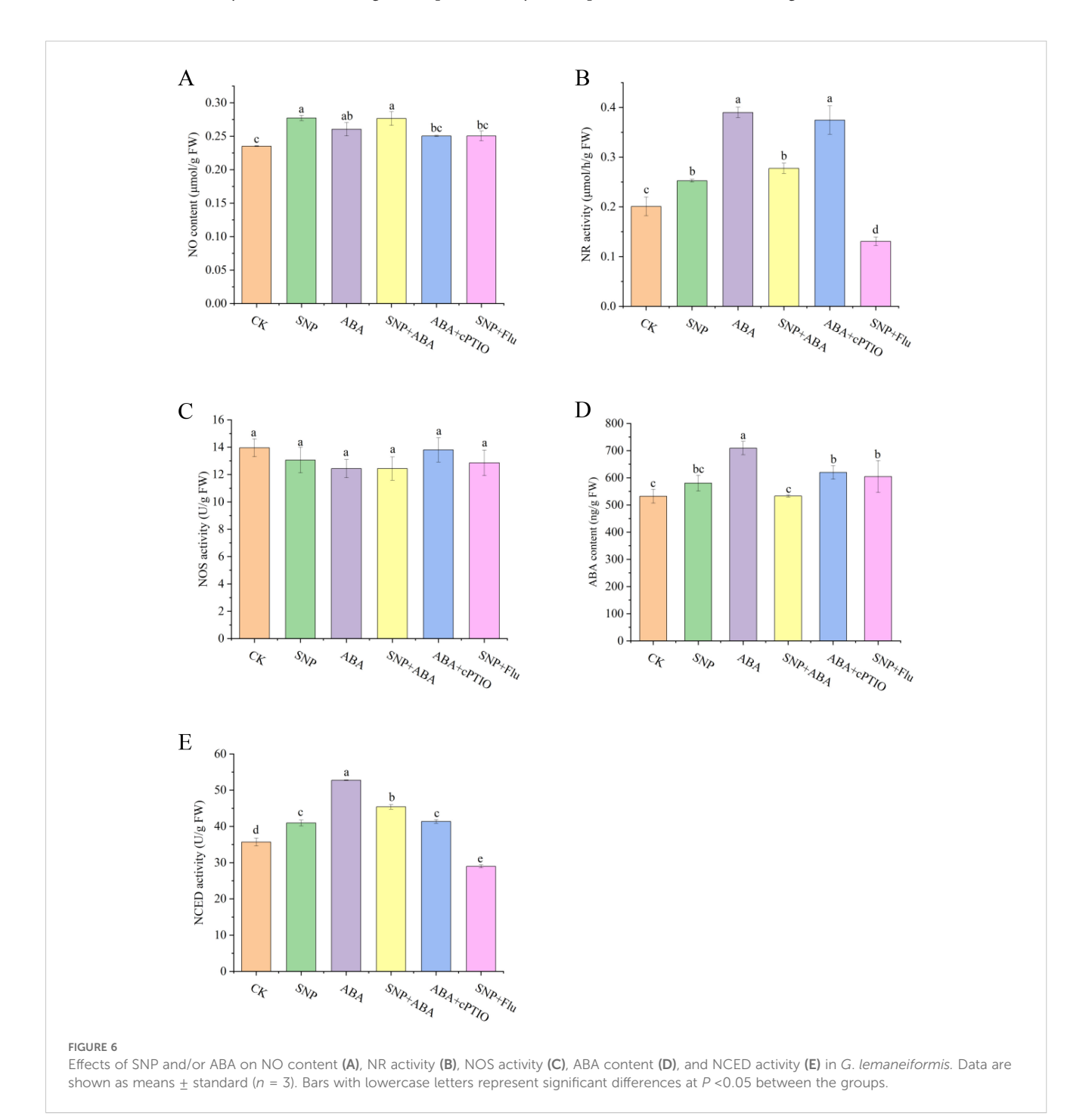
4 Discussion

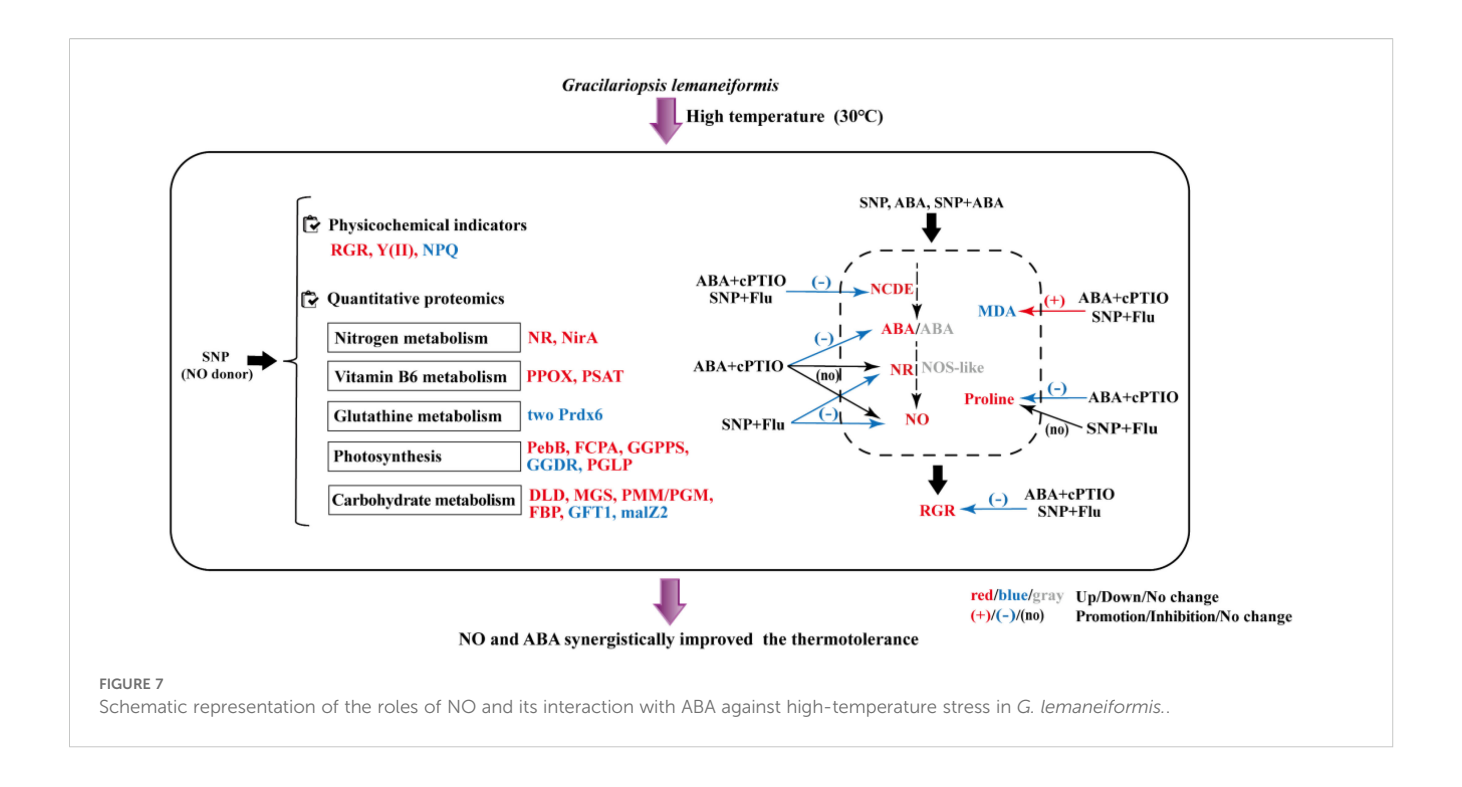
Exogenous stress-resistant substances are crucial in boosting the heat tolerance of plants—for example, the roles of some substances such as γ -aminobutyric acid and chitooligosaccharides in improving stress tolerance at high temperatures have been demonstrated in macroalga *G. lemaneiformis* (Liu et al., 2021; Zhang et al., 2020). NO has also been reported to be effective in strengthening heat resistance in higher plants (Siddiqui et al., 2017); however, no evidence has yet been found in algae. The present study

revealed the positive effects of NO and its synergistic effect with ABA in alleviating the high-temperature stress in *G. lemaneiformis*.

4.1 NO promotes growth and photosynthetic system in plants under high-temperature stress

NO plays a critical role in enhancing plant tolerance against hightemperature stress. NO can mitigate the adverse effects of heat stress





and improve photosynthetic efficiency, resulting in the promotion of plant growth—for instance, the pretreatment of seeds with SNP optimizes seedling growth and their biomasses under heat conditions (Kaur and Kaur, 2018). In addition, the net photosynthesis rate and maximal PSII efficiency were stimulated in high-temperature-stressed wheat (Sehar et al., 2023). In the present study, SNP increased the growth rate and actual PSII efficiency and yet decreased the non-photochemical quenching of *G. lemaneiformis*. NPQ reflects the heat dissipation of plants. Under heat conditions, NO is implicated in the decline of NPQ (Hossain et al., 2011). Similarly, a decrease in NPQ was also observed in the chitooligosaccharide-induced heat tolerance of *G. lemaneiformis* (Zhang et al., 2020).

Except for the effects on the above-mentioned chlorophyll fluorescence parameters, the supply of NO also upregulated the protein levels of photosynthetic pigments such as PebB and GGPPS, whereas it downregulated GGDR in the present proteomics results. PebB acts as a key enzyme in phycoglobin production. GGPPS and GGDR are responsible for the synthesis and degradation of geranylgeranyl pyrophosphate/geranylgeranyl diphosphateare (GGPP/GGDP), respectively. The changes in the protein levels of GGPPS and GGDR ultimately promote the accumulation of GGPP/GGDP, which is a crucial precursor for carotenoid biosynthesis (Chen et al., 2023). Overall, NO promoted the phycobiliprotein and carotenoid synthesis in heat-stressed *G. lemaneiformis*. Similar to this result, NO assisted the chlorophyll content and the expression levels of PSII core protein genes to antagonize the heat damage on photosynthesis in wheat (Sehar et al., 2023).

4.2 NO positively regulates the fundamental metabolisms in plants under high-temperature stress

Carbohydrate metabolism is of great significance to plant growth, development, and stress response. The accumulation of carbohydrates, including total reducing sugar, total carbohydrate content, glucose, fructose, sucrose, and starch, is observed in SNPtreated mustard plants (Sami et al., 2021). In the same way, SNP increases the expression of carbohydrate-metabolism-related proteins in tomato seedlings, thereby alleviating cadmiuminduced programmed death (Huang et al., 2024). In our results, most carbohydrate-metabolism-related proteins, with DLD, FBP, MGS, and PMM/PGM, were upregulated in G. lemaneiformis under heat stress, among which DLD is associated with the tricarboxylic acid (TCA) cycle and photorespiration. Meanwhile, FBP functions in Calvin cycle and sugar partitioning and biosynthesis. In addition, MGS is reported to catalyze the synthesis of exceptionally potent protein stabilizers such as mannosylglycerate (Flint et al., 2005), while PMM/PGM is essential for algal cell wall formation and participates in the biosynthesis of mannose-containing polysaccharides (Zhang et al., 2018a).

Nitrogen metabolism, encompassing nitrogen uptake, utilization, and transformation into amino acid synthesis, is one of the basic physiological processes of plants. In nitrogen metabolism, NR catalyzes the reduction of nitrate to nitrite, while NirA mediates the subsequent conversion of nitrite to ammonia in

plants. Among them, NR serves as the rate-limiting step. A study has shown that SNP enhances heat stress tolerance in pepper by activating NR activity (Zhou et al., 2024). SNP can stimulate the enzyme activities of NR and NiR to mitigate Ni-induced toxicity in cyanobacteria (Singh and Prasad, 2024). Consistent with the abovementioned reports, SNP not only improved NR activity but also upregulated the protein expression levels of NR and NirA in *G. lemaneiformis* at 30°C.

As a coenzyme of many enzymes, vitamin B6 participates in various physiological and metabolic processes such as amino acid metabolism, and its accumulation has been linked to enhanced resistance to biotic or abiotic stresses (Mangel et al., 2019). Enzyme PPOX presents in deoxyxylose 5'-phosphate-independent de novo vitamin B6 biosynthesis pathway, and PSAT participates in the catalytic synthesis of 4-hydroxy-L-threonine (the precursor of vitamin B6 synthesis). Here SNP upregulated the two proteins' expression levels. Moreover, PSAT exhibited a prominent increase (4.29-fold), and PSAT is also involved in the phosphorylation pathway of serine biosynthesis, which is one of the three recognized serine synthesis pathways in plant organisms (Sekula et al., 2018). It has been established that serine contributes to heat stress tolerance (Wang et al., 2024). In summary, NO improved vitamin B6 metabolism and stimulated serine synthesis, which is conducive to boost heat stress tolerance in G. lemaneiformis.

4.3 NO and ABA synergistically mitigate high-temperature stress

The crosstalk between NO and ABA plays important roles in regulating biological stresses such as heat, drought, and salt stress. In terms of heat stress, NO and ABA interact synergistically to maximize osmolyte production as well as the activity and expression of antioxidant enzymes, while cPTIO and Flu addition negates their protective effects (Iqbal et al., 2022). Under drought stress, SNP and/or ABA can elevate proline accumulation and decrease the MDA content in Brassica juncea, with NO independently or the co-application with ABA being more effective than ABA treatment individually (Sahay et al., 2019). In this study, NO and ABA also enhanced the growth and proline level and meanwhile diminished the MDA level. cPTIO or Flu diminished the positive effects of SNP or ABA on growth and MDA contents. As for proline, NO scavenging reduced ABAinduced proline accumulation, but ABA inhibition did not significantly affect the proline level.

ABA can induce the synthesis of endogenous NO; conversely, NO has minimal effects on endogenous ABA synthesis. Studies have demonstrated that NO acts downstream of ABA in the network of NO and ABA signaling pathways (Hancock et al., 2011; León et al., 2014). In *Nitraria tangutorum*, ABA significantly promotes endogenous NO synthesis under arsenic stress, but SNP has little effect on endogenous ABA production (Zhang et al., 2023a). Similarly, in tall fescue, ABA increases NO accumulation under

low-temperature stress by activating NOS activity and upregulating NOS-associated gene expression, whereas NO or cPTIO does not affect endogenous ABA concentration or the transcript levels of ABA receptors (Zhang et al., 2018b). In cold-stored peaches, NO and ABA maintain the NR-induced high levels of NO, and ABA mediates endogenous ABA synthesis by autocatalytic reaction; however, NO does not regulate ABA synthesis (Tian et al., 2020). Consistent with these results, SNP alone and in combination with ABA both stimulated NO accumulation without significantly altering the ABA content. Furthermore, based on the observed changes in proline and MDA contents as well as the NO and ABA levels and their key metabolic enzyme activities, it is speculated that NO might function downstream of the ABA signaling pathway in *G. lemaneiformis* in response to high temperature.

5 Conclusions

This study investigated the role of NO and its crosstalk with phytohormone ABA in enhancing high-temperature resistance in the seaweed G. lemaneiformis. As illustrated in the schematic representation (Figure 7), the application of NO donor SNP improved the photosynthetic parameters and promoted the growth of G. lemaneiformis. Moreover, exogenous SNP upregulated the pathways associated with nitrogen metabolism, vitamin B6 metabolism, and some proteins related to carbohydrate metabolism and photosynthesis (Figure 7). Finally, exogenous NO or ABA supplementation promoted endogenous NO and/or ABA levels and their metabolic enzymes activities. The clearance of NO reduced the NCED activity and ABA content, while the inhibition of ABA synthesis lowered the NR activity and NO level. Consequently, ABA acts upstream of the NO signaling pathway. Meanwhile, NO and ABA demonstrated a synergistic effect on proline accumulation and MDA reduction, resulting in an elevated growth rate. This study will enrich our understanding of the positive roles of NO as well as ABA in improving the hightemperature resistance in algae.

Data availability statement

The raw data supporting the conclusions of this article will be made available by the authors, without undue reservation.

Author contributions

LC: Formal Analysis, Data curation, Writing – original draft. XY: Formal Analysis, Data curation, Writing – original draft. ML: Writing – original draft, Formal Analysis. SL: Methodology, Writing – review & editing, Investigation. NX: Writing – review & editing, Validation, Funding acquisition. XS: Conceptualization, Supervision, Writing – review & editing, Funding acquisition.

Funding

The author(s) declare financial support was received for the research and/or publication of this article. This work was supported by the Key Program of Science and Technology of Ningbo (2019B10009; 2021Z114; 2023Z118).

Conflict of interest

The authors declare that the research was conducted in the absence of any commercial or financial relationships that could be construed as a potential conflict of interest.

Generative AI statement

The author(s) declare that no Generative AI was used in the creation of this manuscript.

Any alternative text (alt text) provided alongside figures in this article has been generated by Frontiers with the support of artificial

intelligence and reasonable efforts have been made to ensure accuracy, including review by the authors wherever possible. If you identify any issues, please contact us.

Publisher's note

All claims expressed in this article are solely those of the authors and do not necessarily represent those of their affiliated organizations, or those of the publisher, the editors and the reviewers. Any product that may be evaluated in this article, or claim that may be made by its manufacturer, is not guaranteed or endorsed by the publisher.

Supplementary material

The Supplementary Material for this article can be found online at: https://www.frontiersin.org/articles/10.3389/fmars.2025. 1635506/full#supplementary-material

References

Bouchard, J. N., and Yamasaki, H. (2008). Heat stress stimulates nitric oxide production in *Symbiodinium microadriaticum*: a possible linkage between nitric oxide and the coral bleaching phenomenon. *Plant Cell Physiol.* 49, 641–652. doi: 10.1093/pcp/pcn037

Chen, D., Wang, Z., Qin, L., Zhang, C., Cao, L., Li, H., et al. (2023). Overexpression of geranyl diphosphate synthase 1 (NnGGPPS1) from *Nelumbo nucifera* enhances carotenoid and chlorophyll content and biomass. *Gene* 881, 147645. doi: 10.1016/j.gene.2023.147645

Chen, Q., Yu, X., Liu, S., Luo, S., Chen, X., Xu, N., et al. (2022). Identification, characteristics and function of phosphoglucomutase (PGM) in the agar biosynthesis and carbon flux in the agarophyte *Gracilariopsis lemaneiformis* (Rhodophyta). *Mar. Drugs* 20, 442. doi: 10.3390/md20070442

Flint, J., Taylor, E., Yang, M., Bolam, D. N., Tailford, L. E., Martinez-Fleites, C., et al. (2005). Structural dissection and high-throughput screening of mannosylglycerate synthase. *Nat. Struct. Mol. Biol.* 12, 608–614. doi: 10.1038/nsmb950

García-Mata, C., and Lamattina, L. (2001). Nitric oxide induces stomatal closure and enhances the adaptive plant responses against drought stress. *Plant Physiol.* 126, 1196–1204. doi: 10.1104/pp.126.3.1196

Hancock, J. T., Neill, S. J., and Wilson, I. D. (2011). Nitric oxide and ABA in the control of plant function. *Plant Sci.* 181, 555–559. doi: 10.1016/j.plantsci.2011.03.017

Hossain, K. K., Nakamura, T., and Yamasaki, H. (2011). Effect of nitric oxide on leaf non-photochemical quenching of fluorescence under heat-stress conditions. *Russ. J. Plant Physiol.* 58, 629–633. doi: 10.1134/S1021443711030046

Huang, D., Chen, X., Yun, F., Fang, H., Wang, C., and Liao, W. (2024). Nitric oxide alleviates programmed cell death induced by cadmium in *Solanum lycopersicum* seedlings through protein S-nitrosylation. *Sci. Total Environ.* 931, 172812. doi: 10.1016/j.scitotenv.2024.172812

Iqbal, N., Sehar, Z., Fatma, M., Umar, S., Sofo, A., and Khan, N. A. (2022). Nitric oxide and abscisic acid mediate heat stress tolerance through regulation of osmolytes and antioxidants to protect photosynthesis and growth in wheat plants. *Antioxidants* 11, 372. doi: 10.3390/antiox11020372

Ji, Z., Zou, D., Gong, J., Liu, C., Ye, C., and Chen, Y. (2019). The different responses of growth and photosynthesis to $\mathrm{NH_4}^+$ enrichments between *Gracilariopsis lemaneiformis* and its epiphytic alga *Ulva lactuca* grown at elevated atmospheric CO_2 . *Mar. pollut. Bull.* 144, 173–180. doi: 10.1016/j.marpolbul.2019.04.049

Kaur, K., and Kaur, K. (2018). Nitric oxide improves thermotolerance in spring maize by inducing varied genotypic defense mechanisms. *Acta Physiol. Plant* 40, 55. doi: 10.1007/s11738-018-2632-9

Kopyra, M., and Gwózdz, E. A. (2004). The role of nitric oxide in plant growth regulation and responses to abiotic stresses. *Acta Physiol. Plant* 26, 459–472. doi: 10.1007/s11738-004-0037-4

Kumar, A., Castellano, I., Patti, F. P., Palumbo, A., and Buia, M. C. (2015). Nitric oxide in marine photosynthetic organisms. *Nitric. Oxide* 47, 34–39. doi: 10.1016/j.niox.2015.03.001

León, J., Castillo, M. C., Coego, A., Lozano-Juste, J., and Mir, R. (2014). Diverse functional interactions between nitric oxide and abscisic acid in plant development and responses to stress. *J. Exp. Bot.* 65, 907–921. doi: 10.1093/jxb/ert454

Lin, H., Ding, J., Peng, Y., Feng, M., and Ying, S. (2022). Proteomic and phosphoryproteomic investigations reveal that autophagy-related protein 1, a protein kinase for autophagy initiation, synchronously deploys phosphoregulation on the ubiquitin-like monjugation system in the mycopathogen *Beauveria bassiana*. mSystems 7, e0146321. doi: 10.1128/msystems.01463-21

Liu, S., Zhang, J., Hu, C., Sun, X., and Xu, N. (2021). Physiological and transcriptome analysis of γ -aminobutyric acid (GABA) in improving *Gracilariopsis lemaneiformis* stress tolerance at high temperatures. *Algal Res.* 60, 102532. doi: 10.1016/j.algal.2021.102532

Mangel, N., Fudge, J. B., Li, K., Wu, T., Tohge, T., Fernie, A. R., et al. (2019). Enhancement of vitamin B6 levels in rice expressing *Arabidopsis* vitamin B6 biosynthesis *de novo* genes. *Plant J.* 99, 1047–1065. doi: 10.1111/tpj.14379

Provasoli, L. (1968). "Media and prospects for the cultivation of marine algae," in *Cultures and Collections of Algae*. Eds. A. Watanabe and A. Hattori*Proc. US-Jpn. Conf* (Japanese Society of Plant Physiologists, Hakone), 63–75.

Rahaman, H., Herojit, K., Singh, L. R., Haobam, R., and Fisher, A. B. (2024). Structural and functional diversity of the peroxiredoxin 6 enzyme family. *Antioxid. Redox Signal.* 40, 759–775. doi: 10.1089/ars.2023.0287

Sahay, S., Khan, E., and Gupta, M. (2019). Nitric oxide and abscisic acid protects against PEG-induced drought stress differentially in *Brassica genotypes* by combining the role of stress modulators, markers and antioxidants. *Nitric. Oxide* 89, 81–92. doi: 10.1016/j.niox.2019.05.005

Sami, F., Siddiqui, H., and Hayat, S. (2021). Nitric oxide-mediated enhancement in photosynthetic efficiency, ion uptake and carbohydrate metabolism that boosts overall photosynthetic machinery in mustard plants. *J. Plant Growth Regul.* 40, 1088–1110. doi: 10.1007/s00344-020-10166-5

Sehar, Z., Mir, I. R., Khan, S., Masood, A., and Khan, N. A. (2023). Nitric oxide and proline modulate redox homeostasis and photosynthetic metabolism in wheat plants under high temperature stress acclimation. *Plants (Basel)* 12, 1256. doi: 10.3390/plants12061256

Sekula, B., Ruszkowski, M., and Dauter, Z. (2018). Structural analysis of phosphoserine aminotransferase (isoform 1) from *Arabidopsis thaliana* the enzyme involved in the phosphorylated pathway of serine biosynthesis. *Front. Plant Sci.* 9. doi: 10.3389/fpls.2018.00876

Siddiqui, M. H., Alamri, S. A., Al-Khaishany, M. Y. Y., Al-Qutami, M. A., Ali, H. M., and Khan, M. N. (2017). Sodium nitroprusside and indole acetic acid improve the

tolerance of tomato plants to heat stress by protecting against DNA damage. *J. Plant Interact.* 12, 177–186. doi: 10.1080/17429145.2017.1310941

Singh, G., and Prasad, S. M. (2024). Synergistic regulation of hydrogen sulfide and nitric oxide on biochemical components, exopolysaccharides, and nitrogen metabolism in nickel stressed rice field cyanobacteria. *J. Plant Res.* 137, 521–543. doi: 10.1007/s10265-024-01530-7

Song, L., Ding, W., Shen, J., Zhang, Z., Bi, Y., and Zhang, L. (2008). Nitric oxide mediates abscisic acid induced thermotolerance in the calluses from two ecotypes of reed under heat stress. *Plant Sci.* 175, 826–832. doi: 10.1016/j.plantsci.2008.08.005

Sun, M., Yang, X., Zhu, Z., Xu, Q., Wu, K., Kang, Y., et al. (2021). Comparative transcriptome analysis provides insight into nitric oxide suppressing lignin accumulation of postharvest okra (*Abelmoschus esculentus* L.) during cold storage. *Plant Physiol. Bioch.* 167, 49–67. doi: 10.1016/j.plaphy.2021.07.029

Sun, P., Chen, Q., Luo, S., Yu, X., Zhang, X., Xu, N., et al. (2022). The role and mechanism of abscisic acid in mitigating the adverse impacts of high temperature in *Gracilariopsis lemaneiformis. J. Appl. Phycol.* 34, 1073–1087. doi: 10.1007/s10811-021-02606-w

Tian, W., Huang, D., Geng, B., Zhang, Q., Feng, J., and Zhu, S. (2020). Regulation of the biosynthesis of endogenous nitric oxide and abscisic acid in stored peaches by exogenous nitric oxide and abscisic acid. *J. Sci. Food Agric.* 100, 2136–2144. doi: 10.1002/jsfa.10237

Wang, Z., Ma, R., Zhao, M., Wang, F., Zhang, N., and Si, H. (2020). NO and ABA interaction regulates tuber dormancy and sprouting in potato. *Front. Plant Sci.* 11. doi: 10.3389/fpls.2020.00311

Wang, X., Wang, J., Zhu, Y., Qu, Z., Liu, X., Wang, P., et al. (2024). Improving resilience to high temperature in drought: water replenishment enhances sucrose and amino acid metabolisms in maize grain. *Plant J.* 119, 658–675. doi: 10.1111/tpj.16783

Xiong, J., Zhang, L., Fu, G., Yang, Y., Zhu, C., and Tao, L. (2012). Drought-induced proline accumulation is uninvolved with increased nitric oxide, which alleviates

drought stress by decreasing transpiration in rice. J. Plant Res. 125, 155–164. doi: 10.1007/s10265-011-0417-y

Yu, J., and Yang, Y. (2008). Physiological and biochemical response of seaweed *Gracilaria lemaneiformis* to concentration changes of N and P. *J. Exp. Ma. Biol. Ecol.* 367, 142–148. doi: 10.1016/j.jembe.2008.09.009

Zhang, J., Cheng, K., Liu, X., Dai, Z., Zheng, L., and Wang, Y. (2023a). Exogenous abscisic acid and sodium nitroprusside regulate flavonoid biosynthesis and photosynthesis of *Nitraria tangutorum* Bobr in alkali stress. *Front. Plant Sci.* 14. doi: 10.3389/fpls.2023.1118984

Zhang, X., Hu, C., Sun, X., Zang, X., Zhang, X., Fang, T., et al. (2020). Comparative transcriptome analysis reveals chitooligosaccharides-induced stress tolerance of *Gracilariopsis lemaneiformis* under high temperature stress. *Aquaculture* 519, 734876. doi: 10.1016/j.aquaculture.2019.734876

Zhang, X., Liu, Y., Liu, Q., Zong, B., Yuan, X., Sun, H., et al. (2018b). Nitric oxide is involved in abscisic acid-induced photosynthesis and antioxidant system of tall fescue seedlings response to low-light stress. *Environ. Exp. Bot.* 155, 226–238. doi: 10.1016/j.envexpbot.2018.07.001

Zhang, X., Ma, M., Wu, C., Huang, S., and Danish, S. (2023b). Mitigation of heat stress in wheat (*Triticum aestivum* L.) via regulation of physiological attributes using sodium nitroprusside and gibberellic acid. *BMC Plant Biol.* 23, 302. doi: 10.1186/s12870-023-04321-9

Zhang, P., Shao, Z., Li, L., Liu, S., Yao, J., and Duan, D. (2018a). Molecular characterisation and biochemical properties of phosphomannomutase/phosphoglucomutase (PMM/PGM) in the brown seaweed *Saccharina japonica. J. Appl. Phycol.* 30, 2687–2696. doi: 10.1007/s10811-018-1460-z

Zhou, Y., Li, Q., Yang, X., Wang, L., Li, X., and Liu, K. (2024). Mitigating high-temperature stress in peppers: the role of exogenous NO in antioxidant enzyme activities and nitrogen metabolism. *Horticulturae* 10, 906. doi: 10.3390/horticulturae10090906